

# Amplified environmental change: Evidence from land-use and climate change in medieval Minorca

Andrea Luca Balbo<sup>1</sup>  | Arnald Puy<sup>2,3</sup>  | Jaime Frigola<sup>4</sup> | Felix Retamero<sup>5</sup> | Isabel Cacho<sup>4</sup> | Helena Kirchner<sup>5</sup>

<sup>1</sup> Research Group Climate Change and Security (CLISEC), KlimaCampus, Center for Earth System Research and Sustainability (CEN), University of Hamburg, Grindelberg 5/7, Hamburg 20144, Germany

<sup>2</sup> Department of Maritime Civilizations, Recanati Institute for Maritime Studies, University of Haifa, 199 Aba Koushy Ave, Mount Carmel, Haifa 3498838, Israel

<sup>3</sup> Geographisches Institut, Universität zu Köln, Zülpicher Strasse 45, Cologne 50674, Germany

<sup>4</sup> GRC Geociències Marines, Departament Dinàmica de la Terra i l'Oceà, Facultat de Ciències de la Terra, Universitat de Barcelona, C/ Martí i Franquès s/n, Campus de Pedralbes, Barcelona 08028, Spain

<sup>5</sup> Arqueologia Agrària de l'Edat Mitjana (ARAE), Departament de Ciències de l'Antiguitat i l'Edat Mitjana, Facultat de Filosofia i Lletres, Universitat Autònoma de Barcelona (UAB), Campus de Bellaterra s/n, 08193 Cerdanyola, Barcelona, Spain

## Correspondence

A. L. Balbo, Research Group Climate Change and Security (CLISEC), KlimaCampus, Center for Earth System Research and Sustainability (CEN), University of Hamburg, Grindelberg 5/7, Hamburg 20144, Germany.

Email: balbo@cantab.net

## Funding information

Institució Catalana de Recerca i Estudis Avançats, Grant/Award Number: ICREA-Academia; Generalitat de Catalunya, Grant/Award Number: grant 2009 SGR 1305; Ministerio de Economía y Competitividad, Grant/Award Numbers: HAR2010-21932-C02 and HAR2013-42195-P; Alexander von Humboldt-Stiftung/Foundation; Marie Curie Intra-European Fellowship of the European Commission, Grant/Award Number: 623098

## Abstract

The debate on human environmental impact has often been locked into cause–effect reasoning, aiming at factoring human impact on top of climatic variability. Here we use evidence from Minorca and the Mediterranean region to show the potential for amplified environmental change emerging from complex feedbacks between climatic and historical events. Alluvial sediments collected in a gully reveal a 14- to 27-fold increase in sediment accumulation rates, leading to the rapid aggradation of the valley floor from approximately AD 1300 onwards. These environmental changes coincided with the Feudal conquest of Minorca (AD 1287) and with the climatic shift from the Medieval Climate Anomaly (MCA, c. AD 900–1300) to the Little Ice Age (LIA, c. AD 1300–1850). This evidence of unprecedented sediment mobilisation, in context with climatic and historical events marking the Mediterranean region, highlights the implications for environmental vulnerability emerging from positive feedbacks between climate and land-use. Understanding such interactions in historical contexts is paramount to increase our capacity for anticipatory learning in the face of rapid climatic, economical, and ecological transformations today.

## KEYWORDS

Climate, Medieval Climate Anomaly (MCA), Little Ice Age (LIA), Mediterranean, Archaeology

## 1 | INTRODUCTION

The potential of human land-use as a strong environment-transforming factor has been broadly recognised in contemporary as well as in historical and archaeological settings. In this context, the Mediterranean has provided a springboard for the study of human environmental impact. Although some scholars have considered climate change to be the major driving factor (Vita-Finzi, 1969), others have regarded humans as the main actors causing landscape transformations (Runnels, 1995). This polarisation of the debate has led the research focus towards the attribution and quantification of respective responsibilities, overshadowing the importance of the complex feedback linkages between anthropic and climatic drivers.

Here we examine this topic from the context of Minorca (Balearic Islands, Spain), where two major historical and climatic shifts overlapped around AD 1300: (a) the conquest of the island by Feudal powers in the framework of the Crusades (AD 1287; Barceló & Retamero, 2005; Bartlett, 1993), leading to a shift towards an economy focused on the cultivation of cereals and vines as well as animal husbandry, and (b) the onset of the climatic period known as the Little Ice Age (LIA, c. AD 1300–1850), which followed the end of the so-called Medieval Climate Anomaly (MCA, c. AD 900–1300; Mann et al., 2009). The Feudal conquest marked the end of the al-Andalus period (AD 902–1287), characterized by the presence of Arab–Amazigh/Berber tribes and clans, the preponderance of irrigation agriculture and the cultivation of oriental plants previously unheard of in the Mediterranean

(Kirchner & Retamero, 2016; Retamero, 2008). The LIA brought about generally colder conditions in the Northern Hemisphere, including changes in patterns of atmospheric circulation (Mann et al., 2009) and a correlated increase in the frequency and intensity of volcanic events (McGregor et al., 2015). Aiming at assessing the environmental effects derived from the alignment of these climatic and historical events, we analyse a sediment sequence collected in a formerly identified Andalusi irrigated area in the gully of Algendar (Southern Minorca; Barceló & Retamero, 2005; Figure 1).

On the basis of a well-constrained chronology, we apply a sedimentological approach mainly based on the study of sediment accumulation rates, the elemental geochemical composition of sediments (i.e., X-ray fluorescence [XRF] core scanning), sediment colour variations, and grain-size analysis. We observe drastic changes in the deposited sequence, which are synchronous with climatic and historical events, suggesting an immediate environmental response in the area.

## 2 | METHODS AND METHOD-SPECIFIC RESULTS

### 2.1 | Radiocarbon dating and age-depth modelling

We implemented Accelerator Mass Spectrometry radiocarbon dating on three samples of charred and noncharred plant remains obtained from transition boundaries within the sediment sequence, marking deposition phases recognised through optical observation (Figure S1, Table S1), and XRF scanning. We calibrated radiocarbon ages to cal years BP (i.e., before AD 1950) and years BC/AD following IntCal13 calibration curve (Reimer et al., 2013; Table S2). Clam 2.2 in the R environment was used to obtain age-depth models (Blaauw, 2010).

For Algendar, we carried out a linear interpolation between the dated levels weighted by the calibrated probabilities iterated 1,000,000 times and with confidence intervals (CI) set at 95%. No sedimentary hiatuses were identified after visual inspection of the core for the section dated (347–237 cm bgl, below ground level; Table S1). The top 77 cm of the sequence were not sampled and ground level was assumed to represent AD 1950. The age-depth model showed a fit of

9.55 and the 95% confidence ranges spanned from 39 to 184 years (average of 114 years), with a time resolution of 38 years every 1 cm between 342 and 301 cm bgl, 4 years every 1 cm between 301 and 237 cm bgl, and 2–3 years every 1 cm between 237 and 0 cm bgl (Figure S2). We defined the onset and end of the MCA (AD 950–1300) and the LIA (AD 1330–1850) in the model output following the chronology given by Cisneros et al. (2016) for Minorca and by Moreno et al. (2011) for the Iberian Peninsula.

The rest of studies on the MCA-LIA transition in the West Mediterranean were selected through a search by topic in the Web of Science webpage (keywords 'Medieval Climate Anomaly,' 'Little Ice Age,' and 'Mediterranean'). We retrieved those studies providing full information on radiocarbon dates, age-depth modelling and palaeoclimatic data. Age-depth models were built following the authors' reported data on the calibration curve used (e.g. marine or terrestrial), proposed onset and end of the MCA-LIA, type of model (e.g. linear, smooth, spline), and reservoir effects, hiatus or age offsets. Each model was iterated one million times with confidence intervals set at 95%.

### 2.2 | Sediment logging and analysis

XRF core scanning was performed at 10 mm resolution on the AVAATECH core-scanner of the CORELAB Laboratory, Faculty of Earth Sciences, University of Barcelona. Previous to scanning, the core was covered with SPEXCerti Pret Ultralene 1 foil (4 µm) to prevent contamination and desiccation under contact with the Rh tube during measurements. In order to detect major and trace elements respectively, exposition times were set at 10- and 25-s, X-ray voltages at 10 and 30 kV, and X-ray currents at 1.4 and 2.0 mA. Intensity data were collected as total counts though processing of raw elemental data using the WIN AXIL package from Canberra Eurisys. Aiming at correcting for porosity changes and unevenness in the sediment surface, and for water condensation under the scanning foil, total counts for each element were normalized by the total counts for all elements at each depth interval following Bahr et al. (2014). We used elemental log-ratios to define diagenetic processes as well as enrichments and depletions of mobile elements against detrital input, following Weltje

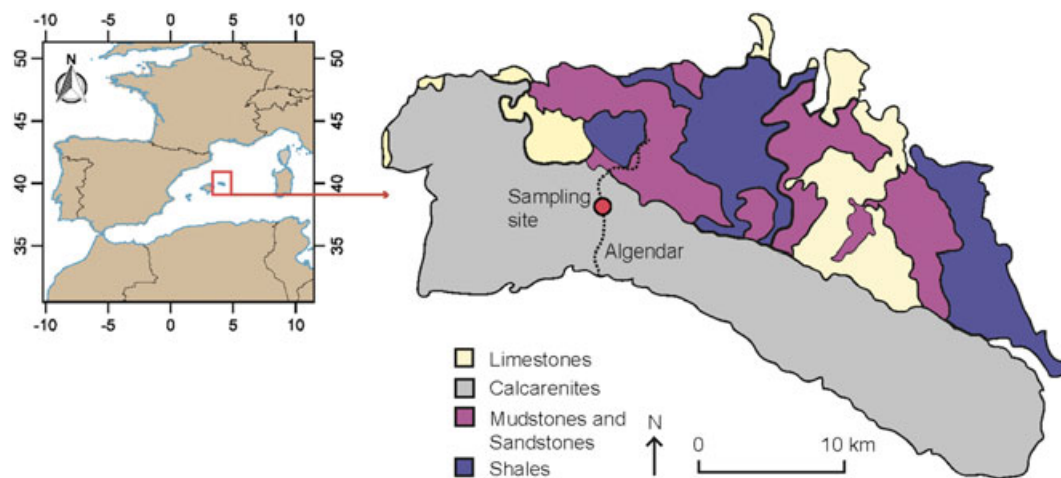


**FIGURE 1** Maps showing the sampling site and the geology of Menorca after Segura, Pardo-Pascal, Rosselló, Fornós, and Gelabert (2007) [Colour figure can be viewed at [wileyonlinelibrary.com](http://wileyonlinelibrary.com)]

and Tjallingii (2008) and Grützner and Higgins (2010). Colour records expressed in CIE-L<sup>\*</sup>a<sup>\*</sup>b<sup>\*</sup> colour space were obtained through image acquisition with the colour line-scan camera integrated in the core scanner allowing (70 µm resolution). We used changes in b<sup>\*</sup> (yellow to blue axis, positive-negative) to describe a lightening of the materials in the Algendar sequence.

Particle size distribution (PSD) analyses were performed in a Coulter LS on discreet samples extracted at regular intervals from the sediment column after removing organic matter with H<sub>2</sub>O<sub>2</sub> (5% solution). We used GRADISTAT version 8.0 (Blott & Pye, 2001) to calculate grain size statistics (Table S3). Because PSD analysis yields compositional data (e.g., vectors formed by positive values that provide portions of a total) (Aitchison, 1982), we used an *i lr*-transformation to overcome the closure effect using the software CoDaPack 2.0 (Comas-Cufí & Thió-Henestrosa, 2011; Egoscue, Pawlowsky-Glahn, Mateu-Figueras, & Barceló-Vidal, 2003). The *i lr*-transformation generates D-1 balances from a sequential binary partition and the resulting variables can be reliably used to perform standard statistical tests such as correlation analyses (Filzmoser & Hron, 2009).

In order to assess how the increase in the sedimentation rates attested in Algendar related to changes in particle size, we balanced [clay, silt | sand] (*i lr* 1) and [clay | silt] (*i lr* 2) in account of the compositional aspect of PSD data, with *i lr* 1 and *i lr* 2, respectively, reflecting the changes in the fine/coarse and clay/silt ratios. The correlation of *i lr* 1 ( $r = 0.81$ ) and *i lr* 2 ( $r = 0.77$ ) with the Zr/Rb ratio indicated that the latter did reflect changes in the sediment texture and could be used as a high-resolution granulometry proxy (Kylander, Ampel, Wohlfarth, & Veres, 2011). Overall, the correlation between the *i lrs*, the accumulation rates, and the Zr/Rb ratio ( $r \geq 0.74$ ) confirmed that the two bursts in sedimentation attested at approximately AD 1289 and AD 1532 were linked to a higher relative presence of sand and silt material ( $r$  between *i lr* 1 and *i lr* 2 = 0.67; Figure S3).

We used Fe and Ti as proxies for the red sandstones and shales of Permian and Triassic origin composing the northern sector of the island, where the upper catchment of the Algendar gully is located. Ti has been documented to be approximately 10 and 3 times higher in shales than in sandstones and carbonates, respectively (Mielke, 1979), while typical Fe levels are approximately 15 and 4 times higher in shales than in limestone and sandstone (De Vos, Tarvainen, Salminen, Reeder, & De Vivo, 2006). In red sandstones, Fe cements the grains together. Given the redox-sensitivity of Fe and Ti being inert, we used the Fe/Ti ratio as a proxy to identify authigenic Fe enrichment due to dissolution, migration and recrystallisation (Croudace & Rothwell, 2015). Diagenesis is a relevant factor conditioning Fe contents along the Algendar sedimentary sequence, as indicated by the fluctuating correlations between Fe and Ti in the identified units (Figure S4). In Unit 1 (c. 290 BC–AD 1293), Fe behaviour is controlled by redox cycles with a comparatively negligent contribution of lithogenic sources, as indicated by the observed positive correlation with Fe/Ti ratio ( $r = 0.92$ ) and negative correlation with Al, Ti, or K ( $r \leq -0.44$ ), which represent the clay detrital fraction. The texture, the colour, and the high Fe and Ti contents point towards shales as the main lithogenic source for Layer 1 (Table S1, Figure S4). However, starting from Unit 2 (>c. AD 1297), the behaviour of Fe is much more controlled by allochthonous factors (correlation with Al, Ti, and

K  $\geq 0.78$ ; Figure S4). The sharp decrease in Fe and Ti documented between Units 2 and 3, jointly with higher Zr/Rb ratios and *i lr* 1 values, suggested lower inputs of clay or Fe-rich minerals and higher deposition of coarser materials between approximately AD 1297 and 1534. This period is also characterized by a shift towards more oxic conditions and higher Fe<sup>3+</sup> precipitation, as shown by higher Fe/Ti ratios (Figure 2). Fe and Ti contents as well as the Zr/Rb ratio increase again in Layer 4b, pointing towards red sandstones as a relevant sediment source between approximately AD 1561 and 1639.

We used Ca as a proxy for the Miocene calcarenites characterising the geology of the southern half of Menorca, formed by sand-size fragments of coral and other marine microorganisms embedded in a matrix formed by small biogenic carbonate fragments and mud (Rosell, Gómez, Elizaga, Sans, & Fullana, 1992). As shown in Figure 1, the Algendar gully is mostly incised within this geological zone. In Layer 2 (c. AD 1297–1412), Ca sharply increases and correlates both with Sr ( $r = 0.93$ ) and the Zr/Rb ratio ( $r = 0.95$ ; Figure S4). This is consistent with a burst in calcarenite deposition: Biogenic calcite from marine microorganisms, which are integrated in the matrix of calcarenites in Minorca, is more enriched in Sr than inorganically precipitated Ca (Haenssler, Unkel, Dörfler, & Nadeau, 2014). Besides, Sr shows a negative correlation with Si in Layer 2 ( $r = -0.59$ ), which allow us to rule-out silicates as a potential Sr source (Kylander et al., 2011). On the other side, the abrupt increase in Ca after Layer 2 suggests a massive input of limestone material, characterised by high Ca contents (De Vos et al., 2006). Finally, yellowness also sharply increases after Layer 1, reflecting a shift from darker (shales) to lighter (calcareous) sediments, and carbonate clasts and concretions abound in the matrix of Layer 2 (Table S1).

### 2.3 | Statistics

We carried out statistical analyses in the R environment (R Core Team, 2016; the code can be made available upon request). We run a principal component analysis (PCA) analysis to summarise the structure of the retained dataset and assess whether layers could be differentiated on the basis of their chemical composition. First, we assessed the presence of multivariate outliers following Filzmoser, Garret, and Reiman (Filzmoser, Garrett, & Reimann, 2005), and the existence of outliers and leverage points in the PCA space by computing the score and orthogonal distances of each observation after Varmuza and Filzmoser (2010). In order to prevent extreme values from spoiling the estimation of the principal components, we ran the PCA on a robust correlation matrix on the basis of the Minimum Covariance Determinant (MCD) estimator of location and scatter using the fast MCD algorithm. The number of retained components for the PCA was selected after cross-validating the data 10,000 times in four segments and visually observing the resulting average values of the variance in a boxplot (Figure S5). All correlation coefficients discussed in the paper and in Supporting Information are robust against outliers and were calculated from robust covariance matrices via the fast MCD algorithm.

The 96% of the variance of the dataset was explained by the first two principal components, and both the variables ( $\cos^2 > 0.92$ ) and the observations (>90% with  $\cos^2 > 0.80$ ) are very well represented in the

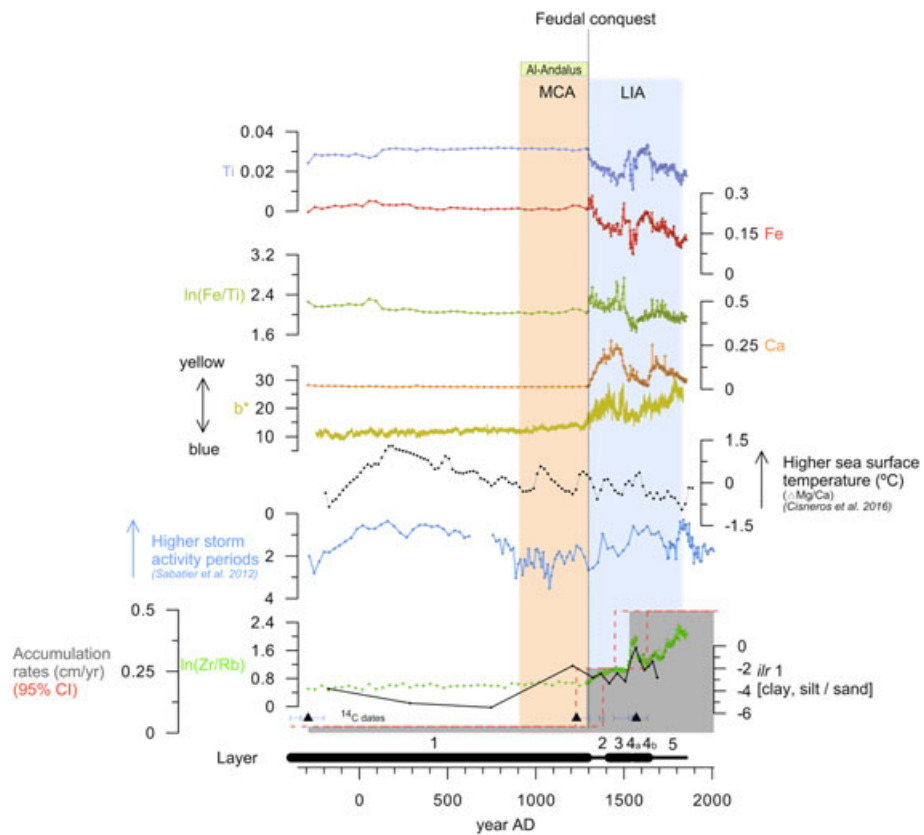


**FIGURE 2** Summary of the main physico-chemical analyses carried out on the Algendar sequence covering the last approximately 2300 years. Results are shown against the AMS dates ( $^{14}\text{C}$  dates plus standard error), the age-depth model, the layers identified in the cores, and the datasets used as temperature and precipitation proxies for the Western Mediterranean and Minorca (Cisneros et al., 2016; Sabatier et al., 2012). Elemental ratios are log-ratios.  $\text{ilr } 1$  reflects the balance [clay, silt | sand] to account for the compositional nature of particle size distribution data (see Supporting Information). Grey bars show the reconstructed sediment accumulation rates [Colour figure can be viewed at [wileyonlinelibrary.com](http://wileyonlinelibrary.com)]

PCA space (Figure S5). PC1 showed high positive loadings of Ca and high negative loadings of Fe and Ti, while PC2 showed high positive loadings of the Zr/Rb ratio and high negative loadings of the Fe/Ti ratio. As can be seen in Figure S5c, all layers appeared clearly differentiated and framed in the corners of the biplot. Layer 1 was characterised by high scores in Fe and Ti, pointing towards a higher presence of shales. A subgroup with higher Fe/Ti values is visible in the plot, indicating that Fe diagenesis might have also been relevant in Unit 1. Layers 2 and 3 showed higher values in Fe/Ti and Ca, evidencing a higher presence of calcarenites and more oxic conditions than in layer 1. Layers 4a and 5 show the highest Zr/Rb ratios and high Ca scores, evidencing their coarsest texture and their enrichment in calcarenites. Finally, Layer 4b showed high Zr/Rb ratios as well as high Ti and Fe scores, pointing towards red sandstones as a major lithogenic component.

We then assessed the extent to which the increase in sedimentation rate and grain size after approximately AD 1300 could be explained by climatic factors. To do so, we compared the Zr/Rb values from Algendar with the storm activity and the sea surface temperatures (SST) datasets by Sabatier et al. (2012) and Cisneros et al. (2016) by means of linear models. For each dataset, we built the linear models using those observations that shared the same best-estimated year with our age depth model (15 observations from the Sabatier et al. dataset, spanning AD 1017–1847; nine observations from the Cisneros et al. dataset, spanning AD 1328–1748).

### 3 | RESULTS SUMMARY

We find that sediment accumulation rates increase in Algendar between AD 1222 and 1306, from approximately  $0.023\text{--}0.028 \text{ cm year}^{-1}$  to  $0.157\text{--}0.538 \text{ cm year}^{-1}$  (95% CI). Sediment accumulation further increases up to approximately  $0.412\text{--}0.623 \text{ cm year}^{-1}$  (95% CI) at the transition between AD 1442–1528 and AD 1551–1634. This is a 5- to 23-fold increase in sedimentation rates between the 13th and 14th centuries AD and a 14- to 27-fold increase from approximately AD 1300 onwards. The burst in sedimentation rates documented in Algendar approximately AD 1300 is linked to the coarsening of the grain size, that is, an approximately 5-fold increase in the relative weight of sand and silt grains within the grain size distribution of the sediment (Figure 2, Figure S3). Two grain-size proxies support this inference: higher  $\text{ilr } 1$  values, which balance [clay, silt | sand] to account for the compositional nature of particle size distribution data (Supporting Information), and higher Zr/Rb ratios (Figure 2). Both proxies are correlated along the core ( $r = 0.81$ ) and indicate an increase in coarse particles supply, likely related to intensified slope erosion starting approximately AD 1300. The occurrence of more intense and frequent erosion events concurred with a sudden change in sediment provenance. Calcarenites, mostly found in the southern half of the island, substitute shales, located to the northern half of Minorca, as the main lithogenic input to the gully after approximately AD 1300 (Figure 1). This is inferred from Ca and Fe-Ti values, used as proxies

for calcarenites and shales, respectively, and from a sharp increase in the yellowness of the materials ( $b^*$ ), reflecting a shift from darker (shales) to lighter (calcareous) sediments (Figure 2). Increased erosion on the lateral slopes and on the surrounding plateaux contributed to the rapid accumulation of sediments at the bottom of the gully, where the studied sequence was recovered. The fast aggradation of the gully floor triggered a rapid change from predominant limnic conditions before approximately AD 1300 to a drier, more oxidized landscape, as indicated by higher Fe/Ti ratios.

## 4 | DISCUSSION

In the Mediterranean, the MCA-LIA transition is related to the establishment of colder temperatures (Cisneros et al., 2016), the recording of higher-frequency variation in water flux and sediment discharge, as described in the Rhône Delta, South France (Arnaud, Revel, Chapron, Desmet, & Tribouillard, 2005), an increase in storminess in the Gulf of Lions, South France (Sabatier et al., 2012; Figure 2), and the occurrence of more acute flood events in the Iberian Peninsula (Benito, Thorndycraft, Rico, Sánchez-Moya, & Sopeña, 2008).

Data collected from a sediment drift, 50 km to the North of Minorca, indicates colder SST during the LIA than during the MCA, particularly in the second half of the LIA. The SST cooling of approximately 1 °C associated to the onset of the LIA, approximately 1300 AD, was relatively short (Figure 2; Cisneros et al., 2016). This marine cooling was coupled with a progressive increase in storm frequency and intensity in the Gulf of Lions (Figure 2; Sabatier et al., 2012), a situation previously correlated to negative North Atlantic Oscillation phases (Cisneros et al., 2016). This atmospheric configuration is consistent with the enhanced intensity in extreme rain events, described for the LIA in the Iberian Peninsula, and with the extreme cold conditions recorded for North Europe during the same period (Mann et al., 2009; Moreno, Valero-Garcés, González-Sampériz, & Rico, 2008).

These general climatic trends are not unequivocally reflected in the elemental composition of the sedimentary sequence of Algendar. Neither Mediterranean SST patterns nor storm activity periods attested in the Gulf of Lions can fully explain the increase in particle size recorded in our sediments after approximately AD 1300. For instance, SST, which is known as being paramount for the development of torrential rain in the region (Pastor, Estrela, Peñarrocha, & Millán, 2001), does not correlate with the Zr/Rb ratio ( $F_{[1, 7]} = 0.557$ , adj.  $r^2 = -0.05$ ,  $p = .479$ ). On the other hand, storminess in the Gulf of Lions explains only half of the Zr/Rb trend observed after approximately AD 1300 ( $F_{[1, 13]} = 16.89$ , adj.  $r^2 = 0.53$ ,  $p = .001$ ). In addition, the beginning of strong erosion-sedimentation events in Algendar predates by approximately 250 years the peaks in storm activity recorded in the Gulf of Lions, attested at approximately AD 1553. Increased precipitation and storminess during the first stages of the LIA led to the development of wetter conditions in some regions of the Western Mediterranean (e.g., Zoñar Lake [Martin-Puertas et al., 2008]; Alborán Sea [Martín-Puertas et al., 2010], and Morocco [Esper et al., 2007]). In Algendar, this trend is masked by the rapid siltation of the gully due to increased erosion and sediment accumulation, with rapid aggradation of the valley floor starting from approximately AD 1300.

The Feudal conquest of Minorca was framed in the process of expansion of the Latin Christendom in Europe, which led to the conquest of Sicily in AD 1090, Jerusalem in AD 1096–1099, and the Baltic regions in the 12th centuries (Bartlett, 1993). Feudal lords took over al-Andalus (Iberian Peninsula) between the 11th and the 15th centuries AD, imposing strong land-use transformations in many areas, including Minorca (Barceló & Retamero, 2005). The overall environmental impact of such process is difficult to assess due to the limited number of paleoenvironmental studies carried out in locations directly involved in the Feudal takeover. For instance, sedimentary records from Lagunillo del Tejo Lake (40 km to the E of Cuenca, Mid-West Spain, conquered in AD 1177; Lopez-Blanco, Gaillard, Miracle, & Vicente, 2012) and Las Tablas de Daimiel wetland (Central Spain, conquered in the 11th century; Gil García et al., 2007), indirectly suggest that the Feudal conquest left weak or no clearly discernible ecological signature in the analysed sedimentary records. Similarly, in the Baltic region, studies aimed at identifying the environmental effects of the Crusades in the late 12th and 13th centuries found no significant changes on rural landscapes and sedimentation patterns (Stivrins et al., 2016).

Besides Algendar, appreciable accelerated sediment deposition rates at the MCA-LIA transition are only found at three other locations within the Western Mediterranean, albeit with considerably lower acceleration values: La Mosca Lake (South Spain, c. 1.5- to 5.5-fold increase; Oliva & Gomez-Ortiz, 2012), Taravilla Lake (Central Spain, c. 7-fold increase; Moreno et al., 2008), and Zoñar Lake (South Spain, c. 3- to 12-fold increase; Martin-Puertas et al., 2008), with the rest of studies showing no significant changes in sedimentation (Figure 3). La Mosca Lake is situated in Sierra Nevada (South of Spain), at 2895 m asl. Although included in a region that was conquered by the Feudals in the 15th century, La Mosca Lake is unlikely to have recorded the environmental impact of the Feudal conquest due to its isolated position. Higher sedimentation rates here may be primarily related to climatic change, their magnitude resulting from the erosion of steep nonvegetated areas. As for Taravilla Lake (30 km to the South of Molina de Segura, conquered by the Feudals in the early 12th century), the relationship between the burst in sedimentation rate, historical and climatic events is difficult to assess due to a crucial sediment gap between AD 1100 and 1400 (Martin-Puertas et al., 2008). Zoñar Lake is, to our knowledge, the only sedimentary record attesting an increase in sedimentation rates partially linked by the authors to the Feudal conquest. Significantly, the conquest of the Guadalquivir basin, where Zoñar Lake is located, was conducted between AD 1224 and 1246, contemporary to the MCA-LIA transition. The Feudal conquest of Minorca (AD 1287) also fully matched the MCA-LIA transition (c. AD 1300). Although a detailed quantification of human environmental impact remains difficult, this comparative overview of available records suggests that, in Mediterranean contexts, even minor land-use changes during the Crusades, such as the introduction of grazing on steep slopes, could have implied an exponential increase in the potential for soil erosion and sediment accumulation given its coupling with the major climatic transition of the time. The resulting effects are comparable to those observed in nonvegetated steep mountain regions. The sedimentological and environmental changes observed in such places as Algendar and Zoñar, therefore, result from a complex process characterised by feedbacks between climatic and historical events and cannot be explained linearly as a sum of these factors.

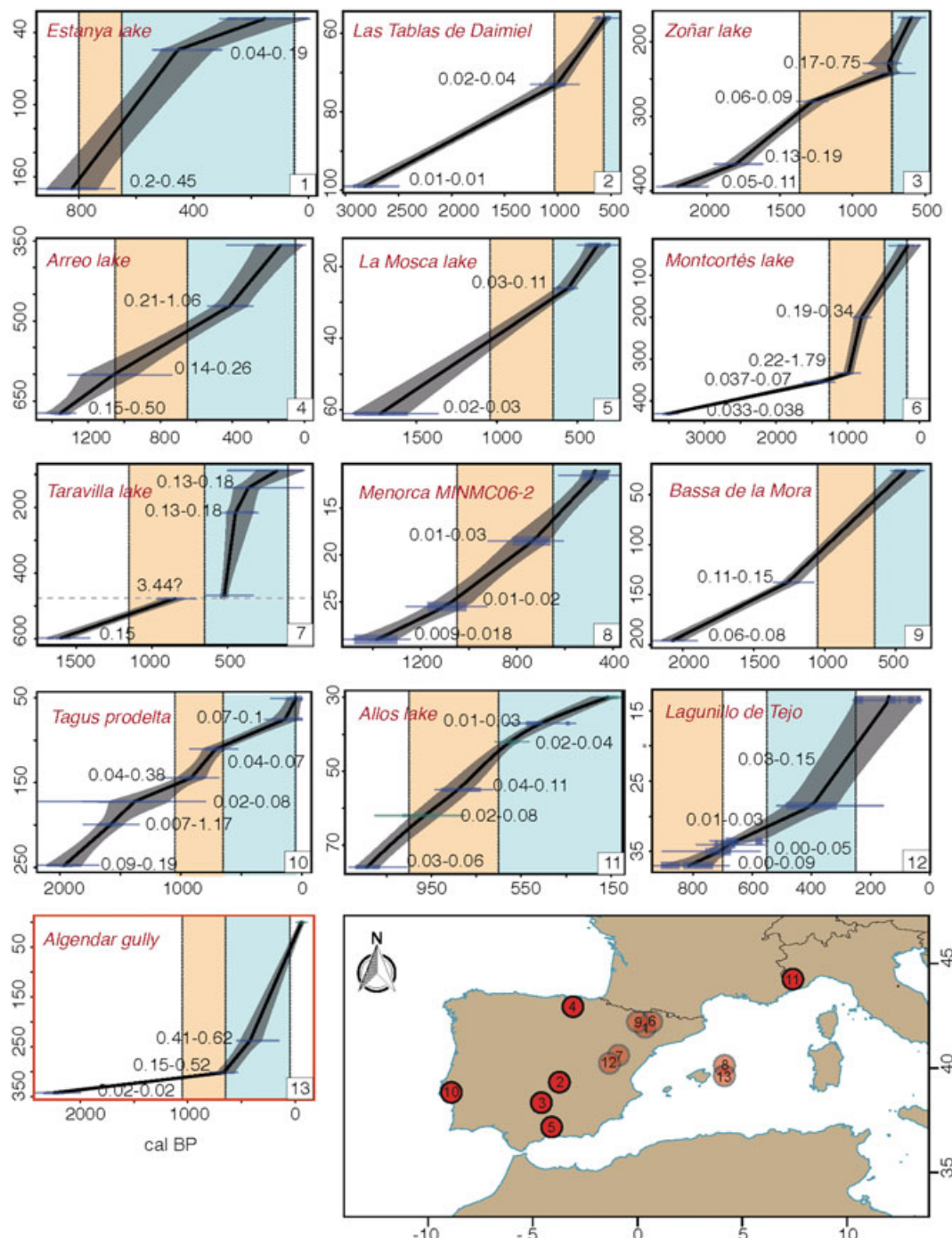


**FIGURE 3** Summary of the age-depth models on the MCA-LIA transition in the Western Mediterranean. For each plot, the timespan of the Medieval Climate Anomaly (orange bar) and the Little Ice Age (blue bar) is defined based on data contained in the cited published works. The best fit and the 95% confidence intervals are shown as a black line and as grey bands, respectively. The numbers in each plot show the 95% CI for the sedimentation rates, expressed as  $\text{cm year}^{-1}$ . Location of each record is shown in the map at the bottom right: (1) Estanya Lake (Morellón et al., 2011), (2) Las Tablas de Daimiel (Gil García et al., 2007), (3) Zoñar Lake (Martin-Puertas et al., 2008), (4) Arreo Lake (Corella et al., 2013), (5) La Mosca Lake (Oliva & Gomez-Ortiz, 2012), (6) Montcortès Lake (Corella et al., 2011), (7) Taravilla Lake (Moreno et al., 2008), (8) Menorca MINMC06-2 (Moreno et al., 2012), (9) Bassa de la Mora (Moreno et al., 2012), (10) Tagus prodelta (Lebreiro et al., 2006), (11) Allos Lake (Wilhelm et al., 2012), (12) Lagunillo de Tejo (Lopez-Blanco et al., 2012), (13) Algendar gully (this study) [Colour figure can be viewed at [wileyonlinelibrary.com](http://wileyonlinelibrary.com)]

## 5 | CONCLUSIONS

Human–environment interactions are complex and characterised by feedbacks acting at different spatial and temporal levels (Barton, 2014). Besides adapting to existing environmental and climatic settings, societal systems actively contribute to the creation of these

environments, which result from reciprocal influences in a continuous human eco-dynamic process (McGlade, 1995). Our study emphasises the implications of paired climatic and land-use change, leading to amplified environmental change as a result of reinforcing positive feedbacks (Meadows, 2009). Such historical case studies provide cautionary tales of the potential unwanted and unpredictable effects of

non-linear dynamics involving complex responses between climatic, environmental, and social–economical processes. Duly studied, they might provide evidence for decisions taken following the precautionary principle, which involves scientific uncertainty and policy-relevant science (Steel, 2015). Historical perspectives, paired with our increased capacity to predict climate change within reasonable uncertainty boundaries, can ultimately inform anticipatory learning in the context of adaptation to current and foreseeable climate change (Tschakert & Dietrich, 2010). Finally, more robust climate adaptive strategies can be defined when the potential amplification effects of human action, aligned with changing climate trends, are taken into account.

## ACKNOWLEDGMENTS

A. L. B. and A. P. worked on this paper with Humboldt Research Fellowships from the Alexander von Humboldt Stiftung/Foundation. A. P. also enjoyed the support of a Marie Curie Intra-European Fellowship (Grant 623098) from the European Commission. This research was sponsored within the framework of projects sponsored by Ministerio de Economía y Competitividad “Productions and agrarian spaces in late medieval Iberian societies. Historical archaeological approaches (12th-16th centuries)” (HAR2013-42195-P; PIs: FR, HK) and “Choices and plant management in al-Andalus. Peasant practices and states” (HAR2010-21932-C02; PI: HK). This research was also partially supported by OPERA project (CTM2013-48639-C2-1-R), Generalitat de Catalunya (Grant 2009 SGR 1305 to GRC Geociències Marines), and Institució Catalana de Recerca i Estudis Avançats (ICREA-Academia Award to IC).

## ORCID

Andrea Luca Balbo  <http://orcid.org/0000-0002-3906-375X>

Arnald Puy  <http://orcid.org/0000-0001-9469-2156>

## REFERENCES

- Aitchison, J. (1982). The statistical analysis of compositional data. *Journal of the Royal Statistical Society. Series B. Methodological*, 44, 139–177. <https://doi.org/10.2307/2345821>
- Arnaud, F., Revel, M., Chapron, E., Desmet, M., & Tribouillard, N. (2005). 7200 years of Rhône river flooding activity in Lake Le Bourget, France: A high-resolution sediment record of NW Alps hydrology. *The Holocene*, 15, 420–428. <https://doi.org/10.1191/0959683605hl801np>
- Bahr, A., Jimenez-Espejo, F. J., Kolasinac, N., Grunert, P., Hernández-Molina, F. J., Röhl, U., ... Alvarez-Zarikian, C. A. (2014). Deciphering bottom current velocity and paleoclimate signals from contourite deposits in the Gulf of Cádiz during the last 140 kyr: An inorganic geochemical approach. *Geochemistry Geophysics Geosystems*, 15, 3145–3160. <https://doi.org/10.1002/2014GC005356>. Received
- Barceló, M., & Retamero, F. (2005). *Els barrancs tancats. L'ordre pagès al sud de Menorca en època andalusina*. Menorca: Institut Menorquí d'Estudis.
- Bartlett, R. (1993). *The making of Europe. Conquest, colonization and cultural change*. London: Princeton.
- Barton, C. M. (2014). Complexity, social complexity, and modeling. *Journal of Archaeological Method and Theory*, 21, 306–324. <https://doi.org/10.1007/s10816-013-9187-2>
- Benito, G., Thorndycraft, V. R., Rico, M., Sánchez-Moya, Y., & Sopeña, A. (2008). Palaeoflood and floodplain records from Spain: Evidence for long-term climate variability and environmental changes. *Geomorphology*, 101, 68–77. <https://doi.org/10.1016/j.geomorph.2008.05.020>
- Blaauw, M. (2010). Methods and code for “classical” age-modelling of radiocarbon sequences. *Quaternary Geochronology*, 5, 512–518. <https://doi.org/10.1016/j.quageo.2010.01.002>
- Blott, S. J., & Pye, K. (2001). Gradistat: A grain size distribution and statistics package for the analysis of unconsolidated sediments. *Earth Surface Processes and Landforms*, 26, 1237–1248. <https://doi.org/10.1002/esp.261>
- Cisneros, M., Cacho, I., Frigola, J., Canals, M., Masqué, P., Martrat, B., ... Lirer, F. (2016). Sea surface temperature variability in the central-western Mediterranean Sea during the last 2700 years: A multi-proxy and multi-record approach. *Climate of the Past*, 12, 849–869. <https://doi.org/10.5194/cp-12-849-2016>
- Comas-Cufí, M., & Thió-Henestrosa, S. (2011). CoDaPack 2.0: a stand-alone, multi-platform compositional software. In J. J. Egozcue, R. Tolosana-Delgado, & M. I. Ortego (Eds.), *CoDaWork'11: 4th International workshop on compositional data analysis*. Sant Feliu de Guíxols.
- Corella, J. P., Moreno, A., Morellón, M., Rull, V., Giralt, S., Rico, M. T., ... Valero-Garcés, B. L. (2011). Climate and human impact on a meromictic lake during the last 6,000 years (Montcortés Lake, Central Pyrenees, Spain). *Journal of Paleolimnology*, 46, 351–367. <https://doi.org/10.1007/s10933-010-9443-3>
- Corella, J. P., Stefanova, V., El Anjoumi, A., Rico, E., Giralt, S., Moreno, A., ... Valero-Garcés, B. L. (2013). A 2500-year multi-proxy reconstruction of climate change and human activities in northern Spain: The Lake Arro record. *Palaeogeography, Palaeoclimatology, Palaeoecology*, 386, 555–568. <https://doi.org/10.1016/j.palaeo.2013.06.022>
- Croudace, I. W., & Rothwell, R. G. (2015). Micro-XRF Studies of Sediment Cores: Applications of a non-destructive tool for the environmental sciences (developments in paleoenvironmental research). Tracking environmental change using lake sediments. *Physical and Geochemical Methods*, 2. <https://doi.org/10.1007/978-94-017-9849-5>
- De Vos, W., Tarvainen, T., Salminen, R., Reeder, S., & De Vivo, B. (Eds.) (2006). *Geochemical Atlas of Europe, part 2. Interpretation of geochemical maps, additional tables, figures, maps and related publications*. EuroGeoSurveys. Brussels: Geological Survey of Finland.
- Egozcue, J. J., Pawlowsky-Glahn, V., Mateu-Figueras, G., & Barceló-Vidal, C. (2003). Isometric logratio transformations for compositional data analysis. *Mathematical Geology*, 35, 279–300. <https://doi.org/10.1023/A:1023818214614>
- Esper, J., Frank, D., Büntgen, U., Verstege, A., Luterbacher, J., & Xoplaki, E. (2007). Long-term drought severity variations in Morocco. *Geophysical Research Letters*, 34. <https://doi.org/10.1029/2007GL030844>
- Filzmoser, P., Garrett, R. G., & Reimann, C. (2005). Multivariate outlier detection in exploration geochemistry. *Computers and Geosciences*, 31, 579–587. <https://doi.org/10.1016/j.cageo.2004.11.013>
- Filzmoser, P., & Hron, K. (2009). Correlation analysis for compositional data. *Mathematical Geosciences*, 41, 905–919. <https://doi.org/10.1007/s11004-008-9196-y>
- Gil García, M. J., Ruiz Zapata, M. B., Santisteban, J. I., Mediavilla, R., López-Pamo, E., & Dabrio, C. J. (2007). Late holocene environments in Las Tablas de Daimiel (south central Iberian peninsula, Spain). *Vegetation History and Archaeobotany*, 16, 241–250. <https://doi.org/10.1007/s00334-006-0047-9>
- Grützner, J., & Higgins, S. M. (2010). Threshold behavior of millennial scale variability in deep water hydrography inferred from a 1.1 Ma long record of sediment provenance at the southern Gardar Drift. *Paleoceanography*, 25, PA4204. DOI: <https://doi.org/10.1029/2009pa001873>
- Haenssler, E., Unkel, I., Dörfler, W., & Nadeau, M. (2014). Driving mechanisms of Holocene lagoon development and barrier accretion in Northern Elis, Peloponnese, inferred from the sedimentary record of the Kotychi Lagoon. *Quaternary Science Journal*, 63, 60–77. <https://doi.org/10.3285/eg.63.1.04>
- Kirchner, H., & Retamero, F. (2016). Becoming islanders. Migration and settlement in the Balearic Islands (10th–13th centuries). In F. Retamero, I. Schjellerup, & A. Davies (Eds.), *Agricultural and pastoral landscapes in pre-industrial society. Choices, stability and change* (pp. 57–78). Oxford and Philadelphia: Oxbow Books.

- Kylander, M. E., Ampel, L., Wohlfarth, B., & Veres, D. (2011). High-resolution X-ray fluorescence core scanning analysis of Les Echets (France) sedimentary sequence: New insights from chemical proxies. *Journal of Quaternary Science*, 26, 109–117. <https://doi.org/10.1002/jqs.1438>
- Lebreiro, S. M., Francés, G., Abrantes, F. F. G., Diz, P., Bartels-Jónsdóttir, H. B., Stroynowski, Z. N., ... Grimalt, J. O. (2006). Climate change and coastal hydrographic response along the Atlantic Iberian margin (Tagus Prodelta and Muros Ria) during the last two millennia. *The Holocene*, 16, 1003–1015. <https://doi.org/10.1177/0959683606hl990rp>
- Lopez-Blanco, C., Gaillard, M.-J., Miracle, M. R., & Vicente, E. (2012). Lake-level changes and fire history at Lagunillo del Tejo (Spain) during the last millennium: Climate or humans? *The Holocene*, 22, 551–560. <https://doi.org/10.1177/0959683611427337>
- Mann, M. E., Zhang, Z., Rutherford, S., Bradley, R. S., Hughes, M. K., Shindell, D., ... Ni, F. (2009). Global signatures and dynamical origins of the Little Ice Age and Medieval Climate Anomaly. *Science*, 326, 1256–1260. <https://doi.org/10.1126/science.1177303>
- Martín-Puertas, C., Jiménez-Espejo, F., Martínez-Ruiz, F., Nieto-Moreno, V., Rodrigo, M., Mata, M. P., & Valero-Garcés, B. L. (2010). Late Holocene climate variability in the southwestern Mediterranean region: An integrated marine and terrestrial geochemical approach. *Climate of the Past*, 6, 807–816. <https://doi.org/10.5194/cp-6-807-2010>
- Martin-Puertas, C., Valero-Garcés, B. L., Pilar Mata, M., Gonzalez-Samperiz, P., Bao, R., Moreno, A., & Stefanova, V. (2008). Arid and humid phases in southern Spain during the last 4000 years: The Zonar Lake record, Cordoba. *The Holocene*, 18, 907–921. <https://doi.org/10.1177/0959683608093533>
- McGlade, J. (1995). Archaeology and the ecodynamics of human-modified landscapes. *Antiquity*, 69, 113–132. <https://doi.org/10.1017/S0003598X00064346>
- McGregor, H. V., Evans, M. N., Goosse, H., Leduc, G., Martrat, B., Addison, J. A., ... Ersek, V. (2015). Robust global ocean cooling trend for the pre-industrial Common era. *Nature Geosciences*, 8, 671–677.
- Meadows, D. H. (2009). *Thinking in systems. A primer*. London: Earthscan.
- Mielke, J. E. (1979). Composition of the Earth's crust and distribution of the elements. In F. R. Siegel (Ed.), *Reviews of research on modern problems in geochemistry* (pp. 13–37). Paris: International Association of Geochemistry and Cosmochemistry, UNESCO.
- Morellón, M., Valero-Garcés, B., González-Sampériz, P., Vegas-Vilarrubia, T., Rubio, E., Rieradevall, M., ... Soto, J. (2011). Climate changes and human activities recorded in the sediments of Lake Estanya (NE Spain) during the Medieval Warm Period and Little Ice Age. *Journal of Paleolimnology*, 46, 423–452. <https://doi.org/10.1007/s10933-009-9346-3>
- Moreno, A., Morellón, M., Martín-Puertas, C., Frigola, J., Canals, M., Cacho, I., ... Valero-Garcés, B. L. (2011). Was there a common hydrological pattern in the Iberian Peninsula region during the Medieval Climate Anomaly? In E. Xoplaki, D. Fleitmann, H. Diaz, L. von Gunten, & T. Kiefer (Eds.), *PAGES news. Medieval Climate Anomaly* (pp. 16–18). <https://doi.org/10.1007/s10933-008-9209-3>
- Moreno, A., Pérez, A., Frigola, J., Nieto-Moreno, V., Rodrigo-Gámiz, M., Martrat, B., ... Valero-Garcés, B. L. (2012). The Medieval Climate Anomaly in the Iberian Peninsula reconstructed from marine and lake records. *Quaternary Science Reviews*, 43, 16–32. <https://doi.org/10.1016/j.quascirev.2012.04.007>
- Moreno, A., Valero-Garcés, B. L., González-Sampériz, P., & Rico, M. (2008). Flood response to rainfall variability during the last 2000 years inferred from the Taravilla Lake record (Central Iberian Range, Spain). *Journal of Paleolimnology*, 40, 943–961.
- Oliva, M., & Gomez-Ortiz A. (2012). Late-Holocene environmental dynamics and climate variability in a Mediterranean high mountain environment (Sierra Nevada, Spain) inferred from lake sediments and historical sources. *The Holocene*, 22, 915–927. <https://doi.org/10.1177/0959683611434235>
- Pastor, F., Estrela, M. J., Peñarrocha, D., & Millán, M. M. (2001). Torrential rains on the Spanish Mediterranean coast: Modeling the effects of the sea surface temperature. *Journal of Applied Meteorology*, 40, 1180–1195. [https://doi.org/10.1175/1520-0450\(2001\)040%3C1180:TROTSM%3E2.0.CO;2](https://doi.org/10.1175/1520-0450(2001)040%3C1180:TROTSM%3E2.0.CO;2)
- R Core Team. 2016. R: A language and environment for statistical computing. Vienna, Austria: the R Foundation for Statistical Computing. ISBN: 3-900051-07-0. Available online at <http://www.R-project.org/>
- Reimer, P. J., Bard, E., Bayliss, A., Beck, J. W., Blackwell, P. G., Bronk, C., ... van der Plicht, J. (2013). IntCal13 and marine13 radiocarbon age calibration curves 0–50,000 years cal bp. *Radiocarbon*, 55, 1869–1887.
- Retamero, F. (2008). Irrigated agriculture, risk and population. The Andalusian hydraulic systems of the Balearic Islands as a case study. In R. Compatangelo-Soussignon (Ed.), *Marqueurs des Paysages et systèmes socio-économiques. Landmarks and socioeconomic systems. Proceedings of Le Mans Cost Conference, 7–9 December 2006* (pp. 135–148). Presses universitaires de Rennes.
- Rosell J, Gómez D, Elízaga E, Sans S, Fullana A. (1992). Mapa geològic de Menorca. OBSAM. Observatori Socioambiental de Menorca.
- Runnels, C. N. (1995). Environmental degradation in ancient Greece. *Scientific American*, 272, 96–99. <https://doi.org/10.1038/scientificamerican0395-96>
- Sabatier, P., Dezileau, L., Colin, C., Briqué, L., Bouchette, F., Martinez, P., ... Von Grafenstein, U. (2012). 7000 years of paleostorm activity in the NW Mediterranean Sea in response to Holocene climate events. *Quaternary Research*, 77, 1–11. <https://doi.org/10.1016/j.yqres.2011.09.002>
- Segura, F. S., Pardo-Pascal, J. E., Rosselló, V. M., Fornós, J. J., & Gelabert, B. (2007). Morphometric indices as indicators of tectonic, fluvial and karst processes in calcareous drainage basins, South Menorca Island, Spain. *Eaarth Surface Processes and Landforms*, 32, 1913–2073. <https://doi.org/10.1002/esp.1506>
- Steel, D. (2015). *Philosophy and the precautionary principle. Science, evidence, and environmental policy*. Cambridge: Cambridge University Press.
- Stivrins, N., Brown, A., Veski, S., Ratniece, V., Heinsalu, A., Austin, J., ... Cerina, A. (2016). Palaeoenvironmental evidence for the impact of the crusades on the local and regional environment of medieval (13th–16th century) northern Latvia, eastern Baltic. *The Holocene*, 26, 61–69. <https://doi.org/10.1177/0959683615596821>
- Tschakert, P., & Dietrich, K. A. (2010). Anticipatory learning for climate change adaptation and resilience. *Ecology and Society*, 15, 11. <http://www.ecologyandsociety.org/vol15/iss2/art11/>
- Varmuza K, Filzmoser P. 2010. Introduction to multivariate statistical analysis in chemometrics. *Applied spectroscopy*. Taylor and Francis. DOI: <https://doi.org/10.1366/000370210791114185>
- Vita-Finzi, C. (1969). *The Mediterranean valleys: Geological changes in historical times*. Cambridge: Cambridge University Press.
- Weltje, G. J., & Tjallingii, R. (2008). Calibration of XRF core scanners for quantitative geochemical logging of sediment cores: Theory and application. *Earth and Planetary Science Letters*, 274, 423–438. <https://doi.org/10.1016/j.epsl.2008.07.054>
- Wilhelm, B., Arnaud, F., Sabatier, P., Crouzet, C., Brisset, E., Chaumillon, E., ... Delannoy, J. J. (2012). 1400 years of extreme precipitation patterns over the Mediterranean French Alps and possible forcing mechanisms. *Quaternary Research (United States)*, 78, 1–12. <https://doi.org/10.1016/j.yqres.2012.03.003>

## SUPPORTING INFORMATION

Additional Supporting Information may be found online in the supporting information tab for this article.

**How to cite this article:** Balbo AL, Puy A, Frigola J, Retamero F, Cacho I, Kirchner H. Amplified environmental change: Evidence from land-use and climate change in medieval Minorca. *Land Degrad Dev*. 2018;1–8. <https://doi.org/10.1002/ldr.2869>